Application Note

April 2023

Utility of Low Frequency (LF) Raman Mapping: Dissolution of Acetaminophen (ACE) Spray Dried Dispersions (SDD)

Nico Setiawan, Ph.D., Andrew Smith, and David E. Bugay, Ph.D.

This application note outlines the evaluation of post-dissolution ACE SDD. The results indicated that in all of the cases studied, ACE remained amorphous upon dissolution if it was intimately mixed in the dispersion. However, phase separation from the polymer allowed ACE to crystallize as expected. Interestingly, the type of polymer used affected the ACE polymorph generated. The mixture of polymorphs was observed in the powder X-ray diffraction (PXRD) result (though it could easily be overlooked), while LF Raman maps showed distinct regions of the different polymorphs. This study demonstrated the utility of LF Raman mapping in elucidating the dissolution mechanism of amorphous dispersions.

Keywords: *Low Frequency Raman, Amorphous, Spray dried dispersion, Dissolution, Crystallization, Polymorphs*

Triclinic Labs
Physical and Analytical Chemistry Expertise
www.TriclinicLabs.com

Introduction

The use of amorphous solid dispersions (ASD) to improve the solubility of poorly soluble compounds has increased significantly as evidenced by multiple marketed products over the last decade [1]. Following the production of a miscible system, which is typically performed via a hot melt extrusion or spray drying process, the performance of an ASD is evaluated by dissolution experiments where supersaturation in solution is monitored within the intended biological transit time. However, crystallization may occur upon exposure to the dissolution media which negates the intended advantage of an ASD. For example, it has been reported that incongruent dissolution of an ASD may occur at high drug loading where the polymer dissolves much more rapidly than the drug, resulting in drug crystallization in the matrix [2]. Therefore, while dissolution experiments are critical to the development of an ASD, analysis of the residual post-dissolution solids must be performed to confirm the dissolution data.

In this study, acetaminophen (ACE) spray dried dispersions (SDD) were generated with four different polymers at 50% drug loading. Dissolution experiments were then conducted on these SDD followed by post-dissolution solids analyses with PXRD and low frequency (LF) Raman mapping. Raman chemical imaging [3] combines the chemical identification capabilities of Raman spectroscopy with the spatial resolution of optical microscopy. An area of interest on a sample can be mapped to differentiate regions based on their chemical composition. Typically, molecular vibrational modes are probed to extract this information; however, LF Raman allows researchers to probe the wavenumber region below 400 cm^{-1}, which corresponds to crystal lattice vibrational modes that are unique to each crystalline polymorph. Herein, LF Raman chemical imaging refers to a collection of Raman spectra collected as a grid of sampled points across the surface of a sample with a spectral range between 0-1000 cm^{-1}.

Instrument and Methods

Acetaminophen spray dried dispersions were generated by creating a 50 mg/mL solution of 50:50 ACE/polymer in methanol followed by spray drying via a ProCepT R&D spray dryer with 0.4 m^3/min inlet gas flow, 75 ºC inlet temperature, 2 bar cyclone gas pressure, 0.3 bar nozzle gas pressure, and 100 rpm pump speed. Polymers used in this study were PVP K30, Eudragit L100, Eudragit L100-55, and HPMCAS MG.

PXRD analysis was carried out using a Rigaku SmartLab with the following parameters: reflection mode, collected at 2°-40º (2θ) at 6 º/min and 0.02º step size spun at 11 rpm, using a Cu tube operated at 50 mA and 40 kV.

Dissolution experiments were conducted by adding 4 mL of phosphate buffered saline pH 7.4 into a vial containing 160 mg of ACE SDD. The vial was placed in a shaker/incubator set at 25 ºC and 100 rpm.
At the specified times, a 1 mL sample was withdrawn, filtered, and followed by high-performance liquid chromatography (HPLC) analysis. HPLC analysis was conducted using an Agilent 1100 with a C18 column (4.6×150 mm and 5 µm particle size), 75:25 water/methanol isocratic mobile phase, 0.5 mL/min, 10 minutes run time, 10 µL injection volume, and detection wavelength of 244 nm.

Low frequency (LF) Raman mapping was carried out on the post-dissolution ACE SDD and LF Raman spectra were collected from reference materials for subsequent chemical image generation utilizing non-negative least squares fitting. The post-dissolution solids were vacuum dried to remove residual water and quench the dissolution process. LF Raman spectroscopy was performed using an Ondax CleanLine™ 853 nm Laser Module and SureBlock™ TR-Probe THz Raman System. The Ondax THz Raman system was paired with a Renishaw inVia™ Qontor™ confocal microscope, equipped with a 1200 lines/mm holographic diffraction grating, a 1-inch charge-coupled device (CCD) detector. Test materials were placed onto a motorized XYZ stage under a long working distance (LWD) 50× microscope objective and analyzed using a 180° backscattering geometry. Individual point spectra were collected using a 1 second exposure time and 16 accumulations over the spectral range from 0 to 1040 cm^{-1} (Raman shift) with a spectral resolution of approximately 3 cm^{-1}. Maps were collected with the same spectral range and resolution, but the exposure time was reduced to 0.5 seconds with a single accumulation at each point. Each map encompassed an area of approximately 100x170 µm with a spatial resolution of 2 µm. Data processing was performed using WiRE 5.5.

Results and Discussion

All ACE SDD studied herein were completely amorphous based on their PXRD patterns (Figure 1). These SDD were also shown to be miscible, at least on the scale of the spot size of the microscope and laser configuration used, based on their LF Raman chemical image (not shown).

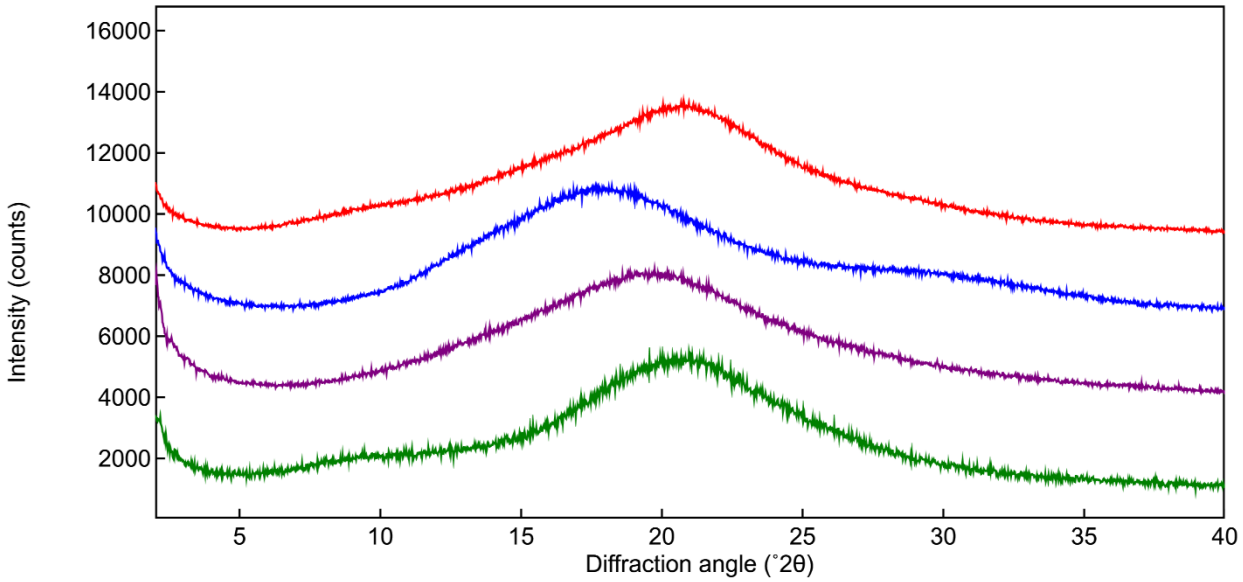

Figure 1. Overlay of PXRD patterns of ACE SDD: 50:50 ACE/PVP K30 (red), 50:50 ACE/Eudragit L100 (blue), 50:50 ACE/Eudragit L100-55 (purple), and 50:50 ACE/HPMCAS MG (green).

The dissolution profile of ACE SDD in the buffer (Figure 2) suggests that PVP resulted in the fastest dissolution rate and highest concentrations throughout the time points compared to other polymers tested in this study (similar dissolution profiles were observed for the remaining polymers).

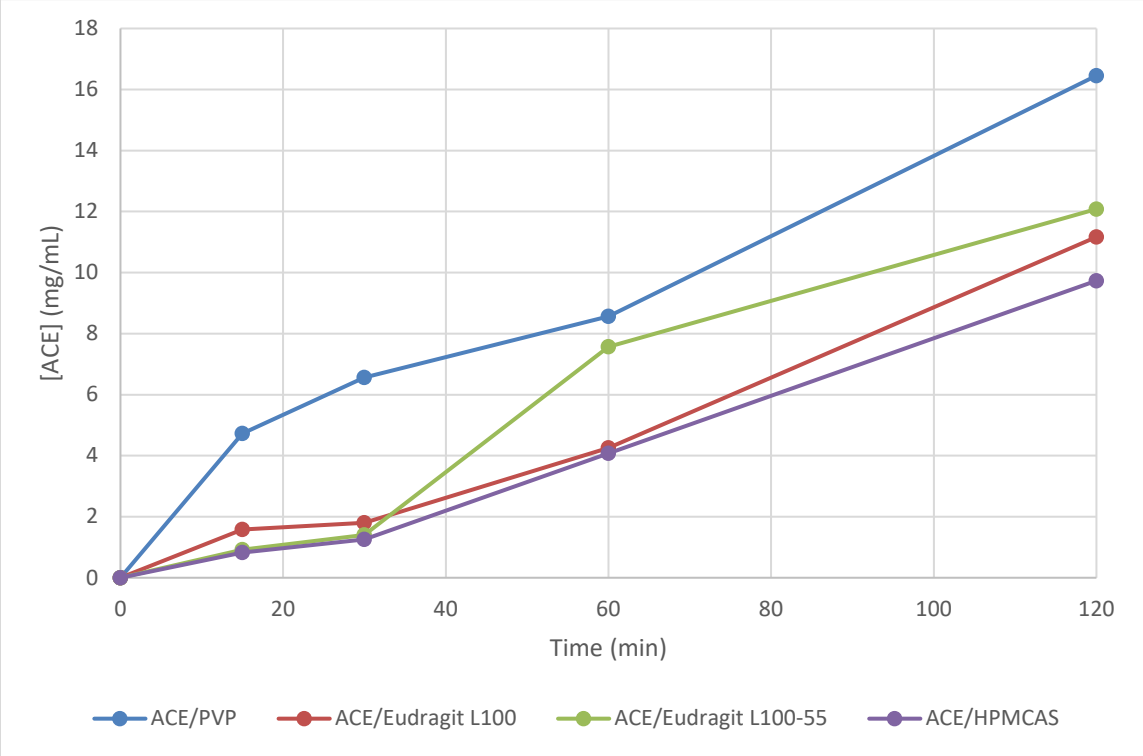

Figure 2. Dissolution profile of various ACE SDD.

Solids remaining at the conclusion of the dissolution experiments were analyzed by PXRD (Figure 3) and LF Raman mapping (Figure 4). The PXRD results showed sharp crystalline peaks from ACE Form I with a raised baseline characteristic of the amorphous phase for all of the post-dissolution solids analyzed. It was also noted that the PVP sample had an additional, though minor peak at 24° characteristic of ACE Form II (see arrow in Figure 3).

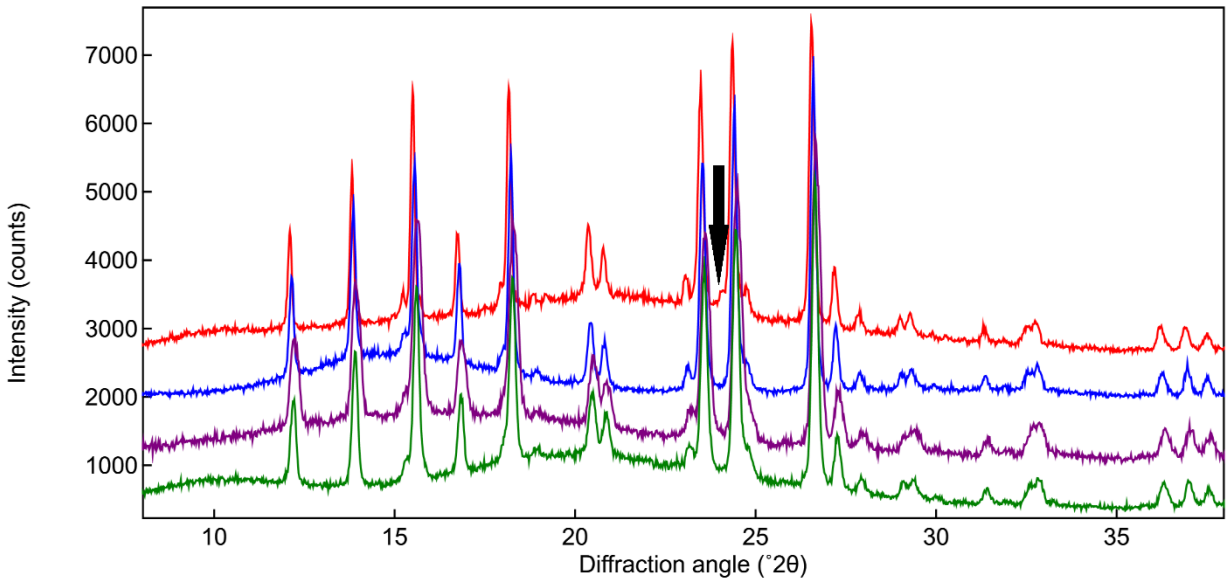

Figure 3. Overlay of PXRD patterns of post-dissolution ACE SDD: 50:50 ACE/PVP K30 (red), 50:50 ACE/Eudragit L100 (blue), 50:50 ACE/Eudragit L100-55 (purple), and 50:50 ACE/HPMCAS MG (green). Black arrow indicates the presence of ACE Form II (see discussion for details).

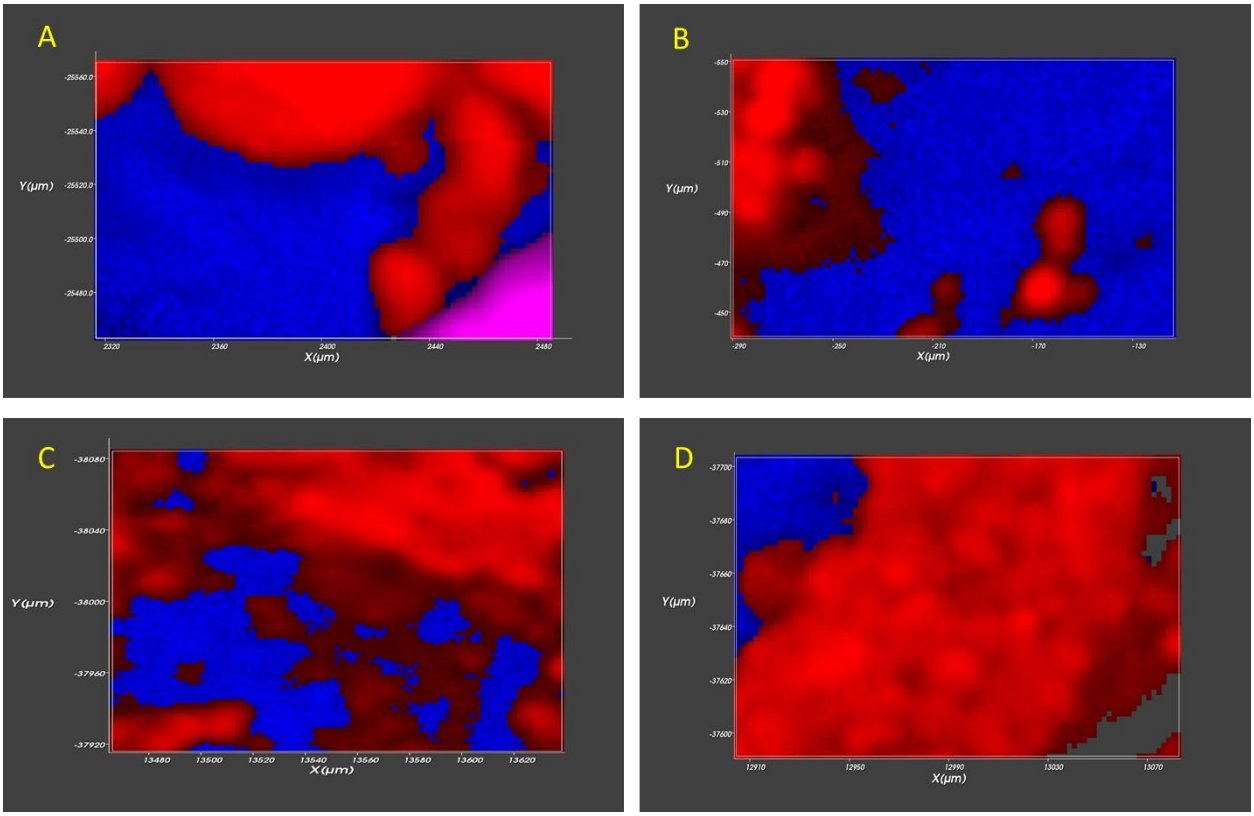

Figure 4. LF Raman chemical image of post-dissolution ACE SDD. (A) 50:50 ACE/PVP K30, (B) 50:50 ACE/Eudragit L100, (C) 50:50 ACE/Eudragit L100-55, and (D) 50:50 ACE/HPMCAS MG. Blue: SDD (amorphous ACE and polymer), red: crystallized ACE Form I, purple: crystallized ACE Form II, dark grey: amorphous ACE.

While PXRD was able to observe all of the phases present in the sample, it is a bulk technique and thus unable to decipher how these phases interact with each other (e.g., what components are there in the amorphous phase? Did crystallization occur in the SDD matrix upon aqueous exposure or did ACE crystallize after dissolving at high concentration?). The LF Raman mapping results, in general, suggest that ACE did not crystallize if it remained in the SDD (the blue area in Figure 4 consists of both amorphous ACE and polymer). However, phase separation from the polymer caused ACE to crystallize, which is expected.

Interestingly, while all SDD crystallized to Form I, PVP SDD also formed ACE Form II crystals. It appears that ACE crystallization occurred because the polymer dissolved and left the SDD matrix rather than crystallizing from the solution. There was no evidence of ACE supersaturation in solution since all of the concentrations measured were below the

equilibrium solubility of ACE Form I, which is 17 mg/mL. It is unknown why Form II was formed in the PVP system, but perhaps the pyrrolidone group, which is a strong hydrogen bond acceptor, disrupted the ACE crystallization process and favored generation of the metastable form instead.

The utility of mapping in the LF Raman range, rather than the more common range of 4000-400 cm^{-1}, is shown in Figure 5 which shows an averaged spectrum of each domain in the post-dissolution PVP SDD sample. The LF Raman chemical images discussed here encompass the LF region at Raman shifts below 400 cm^{-1}, which is sensitive to lattice vibrational mode transitions and thus unique for a given crystal lattice [4,5,6]. The range also extends into the fingerprint region up to 1000 cm^{-1}, which can help differentiate components in cases with good specificity among molecular vibrations of the components. In the case of ACE/PVP, the difference between components (i.e., ACE or PVP) present in a domain was clearly observed through the fingerprint region while, at the same time, the difference between crystal lattices or lack thereof (i.e., ACE Form I, Form II, or amorphous) was observed in the LF region. It is important to note however, that, while a single map area was sufficient to infer the nature of the population for each SDD in this case, additional sampling may be needed for other cases.

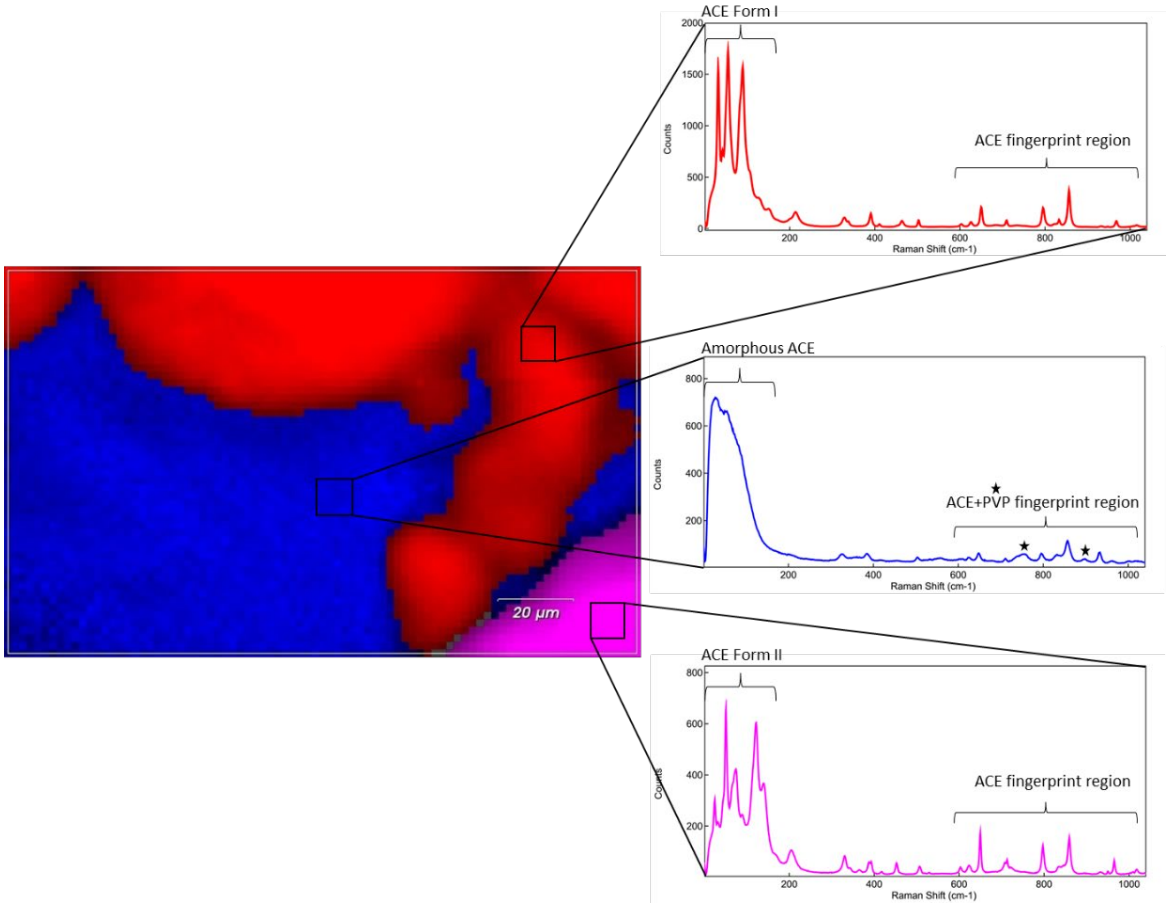

Figure 5. LF Raman spectra in distinct regions observed on post-dissolution ACE/PVP SDD.

Conclusion

The dissolution performance of an amorphous spray-dried dispersion can suffer when exposure to the aqueous media leads to crystallization. Employing LF Raman mapping to produce a chemical image permits evaluation of the post-dissolution solids. In this case, the chemical image provided extensive information on the crystallization behavior of the high drug loading of ACE in the PVP-based SDD.

References

1. DK Tan, et al. AAPS PharmSciTech (2020)21:312. DOI: 10.1208/s12249-020-01854-2.
2. AS Indulkar, et al. Mol Pharm. 2019 Mar 4;16(3):1327-1339. doi: 10.1021/acs.molpharmaceut.8b01261.
3. D.E. Bugay, J-O. Henck, M.L. Longmire, and F.C. Thorley, "Raman Analysis of Pharmaceuticals", in Pivonka, D.E., Chalmers, J.M., and Griffiths, P.R. (Eds.), Applications of Vibrational Spectroscopy in the Pharmaceutical Research and Development, Chichester: John Wiley & Sons, 2007, pp. 239-262.
4. K Berzins, et al. Int. J. Pharm. 2021, 592, 120034. doi.org/10.1016/j.ijpharm.2020.120034.
5. KC Gordon, et al. Spectroscopy 2016, 31(2), 42-50.
6. J Koskela, et al. Mol. Pharmaceut. 2022, 19(7) 2316-2326. doi.org/10.1021/acs.molpharmaceut.2c00126.

Contact Information :

Triclinic Labs
2660 Schuyler Ave., Suite A
Lafayette IN 47905
USA
www.TriclinicLabs.com
rfi@triclinicabs.com